Numerical simulation of unconstrained cyclotron resonant maser emission

2014 J. Phys.: Conf. Ser. 511 012052

(http://iopscience.iop.org/1742-6596/511/1/012052)

Numerical simulation of unconstrained cyclotron resonant maser emission

D. C. Speirs[1], K. M. Gillespie[1], K. Ronald[1], S. L. McConville[1], A. D. R. Phelps[1], A. W. Cross[1], R. Bingham[1,3], B. J. Kellett[3], R. A. Cairns[2] and I. Vorgul[2]

[1] SUPA, Department of Physics, University of Strathclyde, Glasgow, G4 0NG, UK
[2] School of Mathematics and Statistics, University of St Andrews, Fife, KY16 9SS, UK
[3] STFC Rutherford Appleton Laboratory, Chilton, Didcot, Oxfordshire, OX11 0QX, UK

Email: david.c.speirs@strath.ac.uk

Abstract. When a mainly rectilinear electron beam is subject to significant magnetic compression, conservation of magnetic moment results in the formation of a horseshoe shaped velocity distribution. It has been shown that such a distribution is unstable to cyclotron emission and may be responsible for the generation of Auroral Kilometric Radiation (AKR) - an intense rf emission sourced at high altitudes in the terrestrial auroral magnetosphere. PiC code simulations have been undertaken to investigate the dynamics of the cyclotron emission process in the absence of cavity boundaries with particular consideration of the spatial growth rate, spectral output and rf conversion efficiency. Computations reveal that a well-defined cyclotron emission process occurs albeit with a low spatial growth rate compared to waveguide bounded simulations. The rf output is near perpendicular to the electron beam with a slight backward-wave character reflected in the spectral output with a well defined peak at 2.68GHz, just below the relativistic electron cyclotron frequency. The corresponding rf conversion efficiency of 1.1% is comparable to waveguide bounded simulations and consistent with the predictions of kinetic theory that suggest efficient, spectrally well defined radiation emission can be obtained from an electron horseshoe distribution in the absence of radiation boundaries.

1. Introduction

Astrophysical radio emissions in association with plasmas having non-uniform magnetic fields have been the subject of particular interest and debate over the last thirty years [1]. Numerous such sources including planetary and stellar auroral radio emissions are spectrally well defined and exhibit a high degree of extraordinary (X-mode) polarization [2,3] with frequencies of emission extending down to the local relativistic electron cyclotron frequency. In particular, for the terrestrial auroral case it is now widely accepted that such emissions are generated by an electron cyclotron-maser instability driven by a component of the precipitating auroral electron flux having a horseshoe shaped velocity distribution [2]. Such a distribution can form in the precipitating electron stream through conservation of magnetic moment in the convergent magnetic field of the polar magnetosphere and theory has shown that such distributions are unstable to cyclotron emission in the X-mode [4-9].

Figure 1 shows a diagrammatic representation of the formation of a horseshoe distribution in electron velocity space as a result of magnetic compression and the associated evolution in the transverse velocity profile. The velocity space is cut off at $v_{//} = 0$ and does not show the magnetically mirrored component. If one considers the electron beam distribution in figure 1a with finite pitch factor and energy spread impingent on an increasing axial magnetic flux density, conservation of magnetic moment μ results in the conversion of axial velocity into perpendicular velocity. As $v_\perp \propto \sqrt{B_0}$, the resultant expansion in velocity space yields a half-horseshoe like profile (figure 1b) with an increasing number of electrons present at high pitch factors across a positive gradient in the transverse velocity profile ($\partial f_e/\partial v_\perp > 0$). With reference to the analytical theory [4-9], electrons across this positive gradient near the tip of the distribution may undergo resonant energy transfer with an electromagnetic wave and as a result this portion of the distribution will appear to spread in $v_\perp$ and predominantly lose energy.

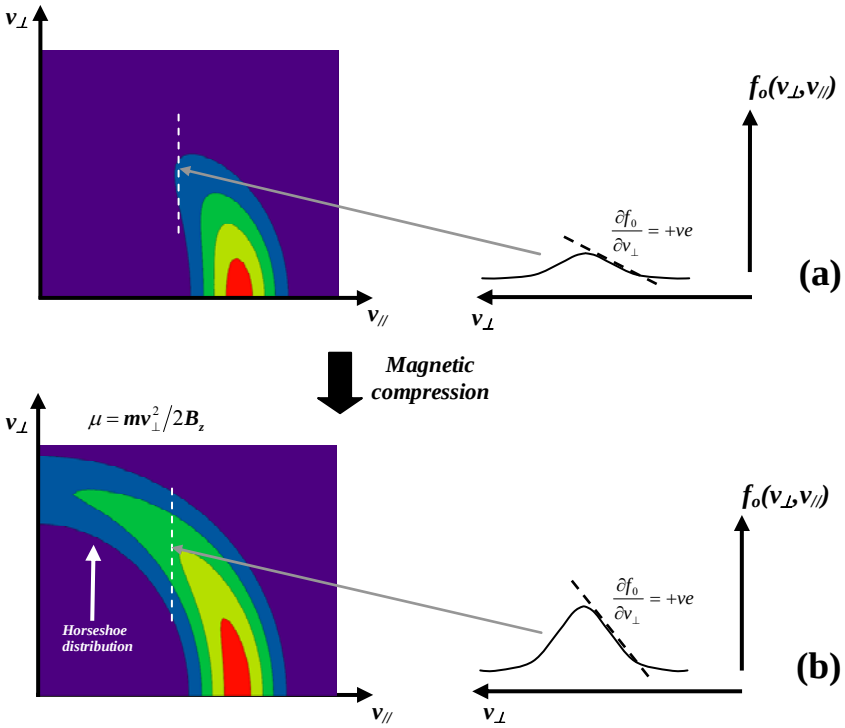

Figure 1. Plots showing the formation and evolution of the horseshoe distribution and transverse velocity profile as the magnetic field is increased from (a) to (b).

2. Numerical Simulations

Previous work at Strathclyde concerned the numerical simulation and laboratory study of the electrodynamics of an electron beam subject to significant magnetic compression within a bounding waveguide structure [10-14]. Cyclotron resonant energy transfer was observed with electromagnetic modes of the waveguide at microwave frequencies [15,16], with RF conversion efficiencies of the order of 1-2%. Here we present the results from PiC (Particle-in-cell) code simulations of the dynamics of the cyclotron emission process in the absence of cavity / waveguide boundaries. Particular consideration was given to the convective growth rate, output spectra and RF conversion efficiencies. In all cases the 2D axisymmetric version of the finite-difference time domain PiC (Particle-in-cell) code KARAT was used. The 2D axisymmetric model allows the distribution of particles in the transverse plane of motion to be monitored via the particle population density in plots of v_ϑ vs v_r. This facilitates the diagnosis of cyclotron-resonant bunching effects in relative electron orbital phase. For the purpose of simulating the unbounded interaction geometry, a 44cm radius region with radially increasing conductivity was defined around the beam propagation path. This represented

an idealised absorber of electromagnetic radiation, inhibiting reflections and hence the formation of boundary resonant eigenmodes. An electron beam was injected into this simulation geometry with a predefined horseshoe distribution, comprising a pitch spread $\alpha = v_\perp / v_z$ of 0→9.5, beam energy of 20keV±5% and beam current of 14A. Other simulation parameters included a uniform axial magnetic flux density of 0.1T, grid resolution of 0.25cm, PiC particle merging factor of $3x10^6$ electrons / PiC particle and a total simulation length (beam propagation path) of 4m.

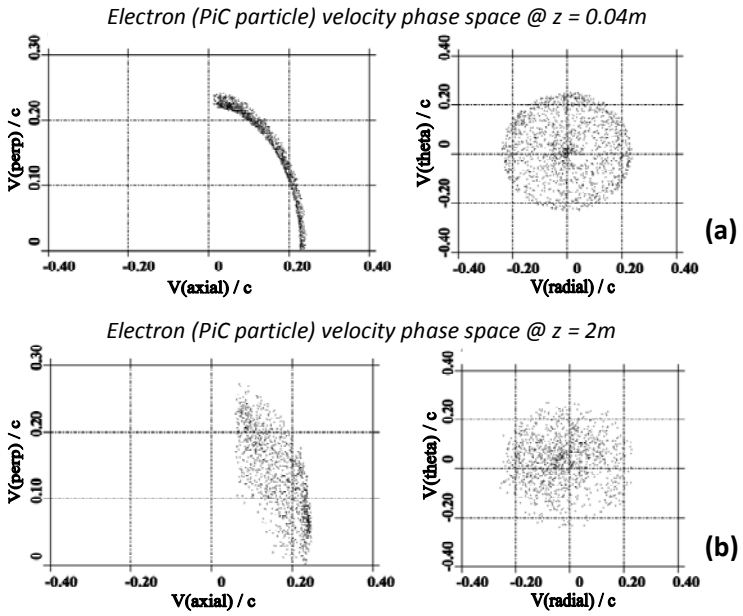

Figure 2. PiC particle velocity distributions measured on transverse planes within the simulation geometry at (a) z = 0.06m and (b) z = 2m

Figure 2 shows the PiC particle velocity distributions at two axial positions within the unbounded simulation geometry after a 200ns run. The injected beam distribution at z = 0.04m contains a well defined pitch spread in $v_\perp$ vs v_z and no evidence of cyclotron bunching effects in the associated v_ϑ vs v_r plot. At an axial position of z = 2m however the picture is very different, with marked smearing in the transverse velocity profile of $v_\perp$ vs v_z over the full pitch range and evidence of electron bunching / phase-trapping in the corresponding v_ϑ vs v_r plot, characterised by a non uniform concentration of PiC particles extending to the origin. Both effects serve as clear evidence for beam-wave energy transfer and the action of a cyclotron maser instability.

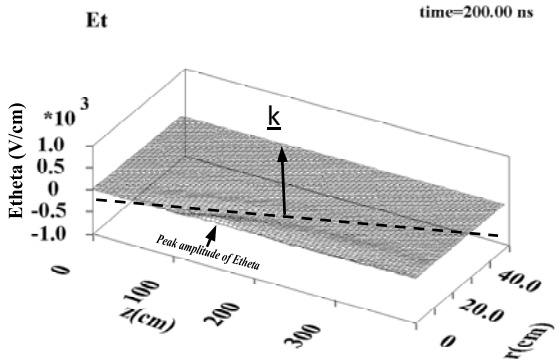

Figure 3. 3D contour plot of E_ϑ within the unbounded simulation geometry.

Figure 3 contains a 3D contour plot of E_ϑ over the simulation geometry after a 200ns run. An electromagnetic wave sourced at z ~ 1.45m is evident propagating near perpendicular to the electron beam with a small backward wave component of the wavevector. A dashed line has been superimposed parallel to the primary wavefront with an arrow indicating the corresponding orientation of the wavevector. A plot of the corresponding radial Poynting flux is presented in figure 4a measured in a plane at r = 3.5cm, over the 4m length of the simulation geometry. A DC offset is present in the measurement due to low frequency electromagnetic field components associated with the electron beam propagation. The rf output power was therefore obtained from the amplitude of the AC signal superimposed on this DC offset. A peak rf output power of ~3kW after 180ns was measured corresponding to an rf conversion efficiency of 1.1%. This is comparable to the ~1% efficiency obtained from waveguide bounded simulations [10-14] and consistent with the estimate of ~1% for the astrophysical phenomena [17,18]. The corresponding output spectrum is presented in figure 4b, showing a well defined signal at 2.68GHz. This represents a 1.1% downshift from the relativistic electron cyclotron frequency of 2.71GHz, consistent with the mild backward wave character observed in figure 3.

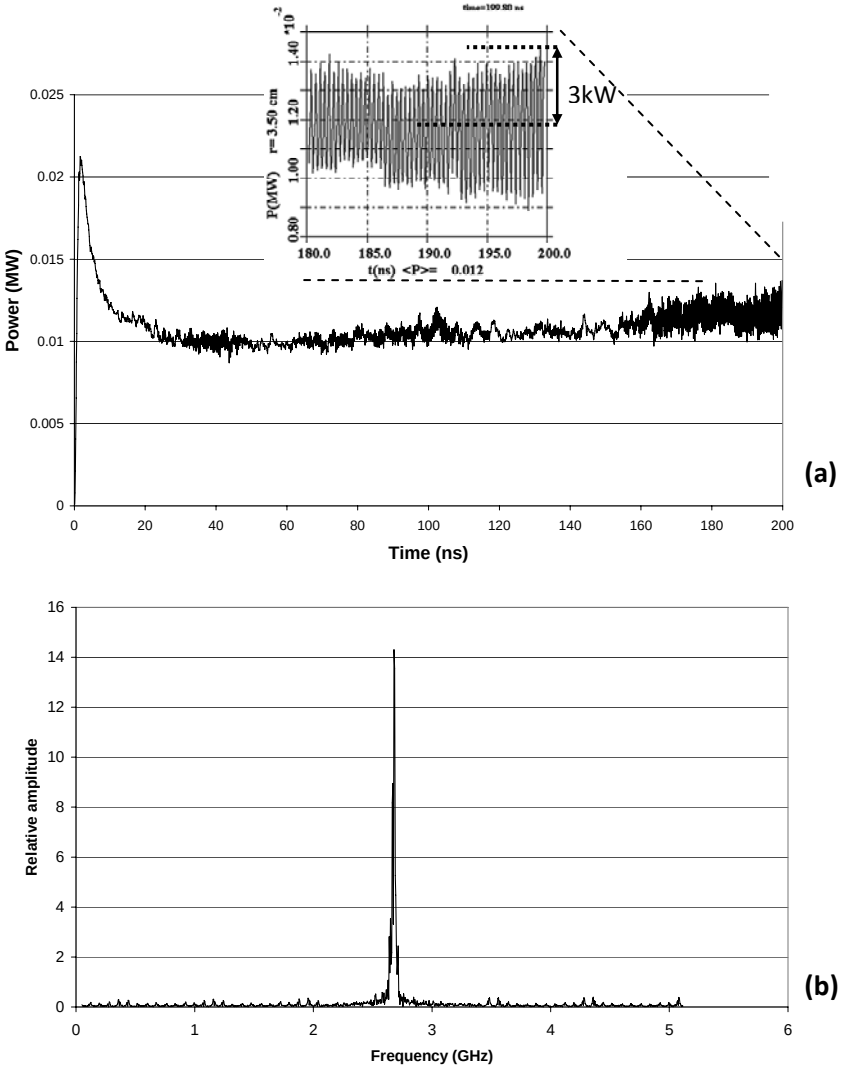

Figure 4. (a) Temporal evolution of the radial Poynting flux measured in a plane at r = 3.5cm spanning the length of the simulation. (b) Fourier transform of E_ϑ from t = 0 →200ns at z = 1.9m.

3. Summary and Conclusions

In conclusion, PiC simulations have been conducted to investigate the dynamics of the cyclotron emission process attributed to numerous astrophysical radio sources [1,17,18] in the absence of cavity boundaries. Computations reveal that a well-defined cyclotron emission process occurs, albeit with a low spatial growth rate compared to waveguide bounded cases [10-14]. RF output is near perpendicular to the electron beam with a slight backward-wave character and well defined spectral output centred just below the relativistic electron cyclotron frequency. The corresponding RF conversion efficiency of 1.1% is comparable to waveguide bounded simulations [10-14] and consistent with the predictions of theory [4-9] and estimates of ~1% for the astrophysical phenomena [17,18].

References

[1] A P. Zarka 1992 *Advances in Space Research*, **12**, 99
[2] D. Gurnett 2008 "Waves in Space Plasmas", *50th Annual APS-DPP Conference*
[3] J.E. Allen & A.D.R. Phelps 1977 *Rep. Prog. Phys*., **40**, 1305-1368
[4] R. Bingham and R. A. Cairns 2000 *Phys. Plasmas*, **7**, 3089
[5] R. Bingham & R.A. Cairns 2002 *Physica Scripta*, **T98**, 160-162
[6] R.A. Cairns et al 2005 Physica Scripta, **T116**, 23-26
[7] D.B. Melrose et al 1982 *J. Geophys. Research: Space Physics* **87,** 5140-5150
[8] R. Bingham et al 2004 *Contributions to Plasma Physics*, **44**, 382-387
[9] I. Vorgul et al 2005 *Physics of Plasmas*, **12**, 1-8
[10] K.M. Gillespie, D.C. Speirs, K. Ronald et al. 2008 *Plasma Phys. Control. Fusion*, **50**, 124038
[11] K. Ronald, D.C. Speirs, S.L. McConville et al. 2008 *Phys. Plasmas*, **15**, 056503
[12] D.C. Speirs et al 2008 *Plasma Physics & Controlled Fusion* **50**, 074011
[13] D.C. Speirs et al 2005 *Journal of Plasma Physics* **71**, 665-674
[14] D.C. Speirs et al 2010 *Physics of Plasmas* **17**, 056501
[15] S.L. McConville et al 2008 *Plasma Physics & Controlled Fusion* **50**, 074010
[16] K. Ronald et al 2008 *Plasma Sources Science & Technology* **17**, 035011
[17] P.L. Pritchett and R.J. Strangeway 1985 *J. Geophys. Res.,* **90**, 9650
[18] D.A. Gurnett 1974 *J. Geophys. Res.,* **79**, 4227